Equivalent: Jurnal Ilmiah Sosial Teknik
Volume 8, Issue 6, 2471-2485
e_ISSN: 2775-0833
https://jurnalequivalent.id/index.php/jequi/index
DOI: doi.org/10.59261/jequi.v8i6.500

Effect of B40 Biodiesel on the Performance and Emissions of Fishing-Vessel Diesel Engines and Its Implications for Operating Costs

Dimas Mahfud Baikuni*
Universitas Muhammadiyah Surakarta, Indonesia

Amin Sulistyanto
Universitas Muhammadiyah Surakarta, Indonesia

***Corresponding author:**
Dimas Mahfud Baikuni Waluyo Adi Siswanto, Universitas Muhammdiyah Surakarta, Indonesia.
✉d200190183@student.ums.ac.id

Article Info:

***Article history*:**
Received: October 16, 2026
Revised: November 04, 2026
Accepted: November 06, 2026
Available Online: November 19, 2026

***Keywords*:**
B40 Biodiesel;
Exhaust Emissions;
Fishing Vessel;
Marine Diesel Engine;
Operating Cost;

This is an open access article under the CC BY-SA license.

Copyright © 2026 by Author. Published by Politeknik Siber Cerdika International

Abstract

Background: Indonesia's B40 mandate (40% palm oil-based fatty acid methyl ester [FAME] blended with petroleum diesel), which took effect in January 2025, extends to fishing fleets that operate older engines and purchase subsidized fuel at a fixed price. However, no study has systematically traced how the blend's fuel properties affect engine behavior and, consequently, fishers' operating costs.
Objective: This study develops and evaluates a closed-form model linking B40 fuel properties to engine performance, exhaust emissions, and trip operating costs across three classes of Indonesian fishing vessels (≤5, 5–10, and 10–30 gross tonnage [GT]).
Methods: A secondary-data modeling approach combines ideal-mixture fuel-property relationships, a Willans-line engine model based on the ISO 8178 E5 marine engine test cycle, exponential emission-response functions, and a trip-level cost function. Uncertainty is propagated through 20,000 Latin hypercube simulation draws, with sensitivity assessed using Sobol indices.
Results: Under the stated model assumptions, B40 reduces volumetric energy content by 3.46%, resulting in a modeled 4.6% increase in fuel volume consumed per trip (90% simulation interval: 2.7–6.6%) and a 2.4–3.0% increase in operating costs. All 20,000 simulation draws yield a positive change in operating costs. Fossil-derived tank-to-wake CO_2 emissions decrease by 37.2%, while modeled CO, HC, and PM emissions decrease by approximately 21–23%. Modeled NO_x emissions increase by 4.9%, although the simulation interval encompasses both a slight decrease and an increase. Cost neutrality requires an estimated compensatory adjustment of Rp347–364 per liter.
Conclusion: At the assumed fixed retail fuel price, B40 imposes an additional modeled cost burden, which is described in this study as an implicit levy solely as an economic metaphor rather than as an official tax or government-imposed charge. The findings underscore the need for field-based engine-efficiency measurements and further policy assessments of potential targeted compensation as Indonesia considers adopting higher biodiesel blends.

To cite this article: Baikuni, D. M. & Sulistyanto, A. (2026). Effect of B40 biodiesel on the performance and emissions of fishing-vessel diesel engines and its implications for operating costs. *Equivalent: Jurnal Ilmiah Sosial Teknik*, *8*(6), 2471-2485. https://doi.org/10.59261/jequi.v8i6.500

INTRODUCTION

The energy transition in Indonesia's capture fisheries is unfolding through the fuel used by fishing vessels. Since January 1, 2025, Indonesia has mandated a 40% palm-oil-based biodiesel blend (B40) for both subsidized and nonsubsidized diesel fuel Kementerian ESDM (2025), and

policy discussions in 2026 have shifted toward B50 (Listrik Indonesia, 2026). The program is intended to reduce diesel imports, absorb domestic palm oil production, and decrease dependence on fossil fuels (Wirawan et al., 2024). Existing Indonesian biodiesel studies cited herein have focused primarily on macroeconomic effects, policy financing, road-vehicle testing, fuel properties, and engine emission responses; they do not directly quantify the effects of B40 on trip-level fuel consumption and operating costs for small fishing vessels. Accordingly, the present study addresses this micro-level research gap specifically in the context of Indonesian fishing-vessel operations. A nominal fuel price of Rp6,800 per liter is subsequently used as a modeling scenario rather than presented as a universally applicable price for all fishing vessels.

Fishers' exposure to fuel-related changes is structural because fuel represents a major variable cost in motorized capture fisheries. A global cost database identifies fuel as a dominant cost component Lam et al. (2011), while studies of fuel intensity demonstrate substantial variation across fishing gear types and stock conditions (Lam et al., 2011; Tyedmers et al., 2005). Using a global fleet assessment covering the period examined in their study, Parker et al. (2018) estimated annual fuel consumption at approximately 40 billion liters and associated greenhouse gas emissions at approximately 179 million tonnes of CO2-equivalent. These global estimates establish the scale of fisheries' dependence on fuel but are not used to infer the magnitude of B40-related effects in Indonesia. The impacts in Indonesia depend on local vessel characteristics, operating intensity, engine condition, and administered fuel-pricing arrangements. The present model evaluates these effects through representative vessel scenarios.

From an engineering perspective, the effects of biodiesel are heterogeneous across engine types and test conditions. Biodiesel has a lower heating value approximately 12–13% below that of conventional diesel on a mass basis, along with higher density, a higher cetane number, and an oxygen content of approximately 11% by mass (Hoekman et al., 2012; Knothe, 2005). Palm methyl ester is relatively saturated and exhibits good oxidative stability but has a comparatively high cloud point (Kalam & Masjuki, 2002; Ong et al., 2011). Reviews generally report increased brake-specific fuel consumption (BSFC) as heating value decreases, whereas brake thermal efficiency (BTE) remains unchanged or decreases modestly (Atabani et al., 2012). Carbon monoxide (CO), hydrocarbons (HC), and particulate emissions often decrease because oxygenated fuels can promote more complete combustion. However, the response of nitrogen oxides (NOx) is less consistent. A higher bulk modulus can advance fuel injection timing, reduced soot radiation can alter in-cylinder temperatures, and shifts in combustion phasing can create conditions favorable to NOx formation (Mokhtar et al., 2023). Nevertheless, the direction and magnitude of NOx responses vary with engine architecture, injection system, biodiesel composition, engine load, calibration, and whether testing is conducted under steady-state or transient conditions (Giakoumis et al., 2012). Accordingly, the emission-response coefficients used in this study are treated as literature-derived approximations, and their applicability to Indonesian fishing-vessel engines is examined through uncertainty ranges rather than assumed to be universal.

For 40% palm-oil-based biodiesel blends, the available empirical evidence remains dominated by road-vehicle applications and controlled engine testing. A national 50,000-km road test reported no major technical problems in the vehicles tested Mokhtar et al. (2023), while engine tests involving palm-oil-based biodiesel blends have reported increased NOx emissions and decreased CO and HC emissions under specific test configurations (Musthafa & Prabhahar, 2025). Fishing-vessel operations differ materially from road-vehicle applications: marine engines may operate for extended periods under sustained or variable propeller loads; fuel may remain in onboard tanks for longer periods; humidity and water contamination present more significant concerns; small-vessel fleets may include older engines equipped with mechanical fuel-injection systems; and fuel-system failures at sea have different operational consequences from roadside failures. High biodiesel blend

concentrations also present concerns regarding filterability, cold-flow properties, water absorption, microbial growth, oxidative stability, and material compatibility (Haryono et al., 2025; Haseeb et al., 2011; Passman, 2013; Pramudito et al., 2023). These differences justify a vessel-specific modeling application while also limiting the direct transferability of emission and performance coefficients derived from road-engine studies to marine fleets.

Within the body of literature reviewed in this manuscript, three related research gaps

motivate the present analysis. First, the available evidence on B40 is concentrated on road vehicles, laboratory engine testing, and general assessments of marine feasibility rather than the trip-level cost implications for Indonesian fishing vessels. Second, engineering studies typically report engine performance and emissions without translating their findings into the operating-cost measures relevant to fishers, whereas the Indonesian policy studies cited herein focus primarily on macroeconomic considerations (Halimatussadiah et al., 2021; Sahara et al., 2022). Third, the studies reviewed do not provide an integrated, closed-form accounting framework that distinguishes among volumetric-energy, combustion-efficiency, and maintenance contributions to fishing-vessel operating costs while accounting for parameter uncertainty. This claim is therefore restricted to the literature examined in developing the present model and is not intended to imply an exhaustive absence of such frameworks across all published research.

This study addresses these gaps through a coupled fuel-property, engine-performance, emission, and cost model evaluated using the ISO 8178 E5 marine test cycle for three representative fishing-vessel classes. Its contributions are threefold. First, the convex relationship between biodiesel blend fraction and volumetric fuel requirements is established as a mathematical proposition derived from the model's stated assumptions. Second, the application of the coupled framework and a break-even compensation metric to Indonesian fishing-vessel classes constitutes a context-specific methodological contribution. Third, the Sobol decomposition integrates an established sensitivity-analysis method to identify the uncertain parameters that most strongly influence modeled operating costs, thereby informing measurement priorities. The primary objective is to estimate the effects of B40 on modeled fuel consumption, BSFC, BTE, and exhaust emission indicators. A secondary objective is to estimate the resulting operating-cost implications and break-even fuel-price offsets and to discuss, rather than presume, their policy relevance in the context of a potential transition toward B50.

METHOD

This study employed quantitative mathematical modeling and stochastic simulation based exclusively on secondary data. Parameter inputs were drawn from fuel-property studies, engine and emission reviews and experiments, ISO/IMO test standards, and Indonesian policy and price sources cited in the manuscript. Source selection was purposive rather than systematic: foundational technical references were retained where they defined physical properties or established models, while recent studies published through 2026 were prioritized for B40/B50 policy developments, high-blend behavior, and validation evidence. Parameters were included when they provided a value, range, or functional relationship required by the fuel-property, Willans-line, emission-response, maintenance, or cost equations. Because the study did not employ a preregistered systematic search protocol, the literature base should be understood as a model-parameter evidence set rather than a systematic review. The study did not involve human or animal participants. The equations, nominal parameters, distributions, and simulation settings reported below were provided to support reconstruction of the analysis. However, because no public computational-code repository accompanied this version, the manuscript did not claim full code-level replicability.

Blend properties at biodiesel volume fraction x were calculated using ideal mixing rules. Density was assumed to mix linearly by volume, whereas the lower heating value (LHV) was assumed to mix linearly by mass fraction w (Equation 1). Consequently, the volumetric energy content Ev was linear in x and could be expressed using a single energy-deficit parameter for neat biodiesel, θ (Equation 2). The nominal values were ρD = 0.835 kg/L and LHVD = 42.9 MJ/kg for diesel, and ρB = 0.875 kg/L and LHVB = 37.4 MJ/kg for palm methyl ester (Hoekman & Robbins, 2012). Here, x denoted the volumetric fraction of fatty acid methyl ester (FAME) in the marketed blend (e.g., x = 0.40 for B40), whereas w denoted the corresponding FAME mass fraction after density conversion. These two quantities were not interchangeable because FAME and petroleum diesel have different densities.

$$\rho_x = (1-x)\,\rho_D + x\,\rho_B, \qquad w = \frac{x\,\rho_B}{\rho_x}, \qquad \mathrm{LHV}_x = w\,\mathrm{LHV}_B + (1-w)\,\mathrm{LHV}_D \tag{1}$$

$$E_v(x) = \rho_x\,\mathrm{LHV}_x = (1-x)\,E_{v,D} + x\,E_{v,B} = E_{v,D}\,(1-x\theta), \qquad \theta = 1 - \frac{E_{v,B}}{E_{v,D}} \tag{2}$$

The engine was modeled using the Willans-line approach. Fuel power in mode j was calculated as the sum of brake power Pb and friction power divided by the indicated efficiency ηi (Equation 3). Friction power was assumed to be proportional to the square of relative engine speed, with a fraction φ of rated power Pr. The effect of biodiesel on combustion quality was represented by a relative efficiency change δη, which was scaled linearly with x. The operating profile followed the ISO 8178 E5 cycle for engines installed on vessels shorter than 24 m. The cycle comprised five modes (100%, 75%, 50%, 25%, and 0% load, corresponding to 100%, 91%, 80%, and 63% rated speed, respectively, and idle), with time weights Wj = 0.08, 0.13, 0.17, 0.32, and 0.30 (International Organization for Standardization [ISO], 2020). Fuel volume per trip V was calculated from the cycle-averaged fuel energy, engine operating hours per trip h, and Ev (Equation 4).

$$\dot{Q}_{f,j} = \frac{P_{b,j} + \phi\, P_r \left(n_j / n_r\right)^2}{\eta_i(x)}, \qquad \eta_i(x) = \eta_{i,0}\left(1 + \delta_\eta \frac{x}{0.4}\right) \tag{3}$$

$$\bar{Q}_f = \sum_{j=1}^{5} W_j\, \dot{Q}_{f,j}, \qquad \bar{P}_b = \sum_{j=1}^{5} W_j\, P_{b,j}, \qquad V(x) = \frac{\bar{Q}_f\, h}{E_v(x)} \tag{4}$$

Emissions of species k ∈ {NOx, CO, HC, PM} were modeled using an exponential response to biodiesel volume fraction, with coefficients ak calibrated from meta-reviews (Xue et al., 2011). Baseline NOx emission factors were based on the IMO Tier I limits as a function of rated engine speed (International Maritime Organization [IMO], 2008). CO_2 was calculated as fossil tank-to-wake emissions, accounting only for the diesel mass fraction, with a carbon mass fraction of cD = 0.865 (Equation 5). Operating cost per trip C comprised fuel costs; filter and lubricating-oil costs, with replacement intervals shortened by factors γ and λ, respectively; annual tank and water-separator housekeeping costs H, allocated across the number of annual trips Nt; and nonfuel costs Cnf, calibrated so that the fuel-cost share at B0 equaled sf (Equation 6). The housekeeping costs reflected the risks associated with water contamination and microbial growth in the marine environment Fregolente et al. (2012) whereas the assumption of more frequent filter replacement was based on evidence concerning the filterability of high palm-oil biodiesel blends.

$$M_k(x) = e_{k,0} \exp(100\, a_k\, x) \bar{P}_b\, h, \qquad M_{\mathrm{CO_2}}(x) = \rho_x V(x)\,(1 - w)\, c_D\, \frac{44}{12} \tag{5}$$

$$C(x) = p\, V(x) + h\left[\frac{c_{fl}\,(1 + \gamma x/0.4)}{T_{fl}} + \frac{c_{oil}\,(1 + \lambda x/0.4)}{T_{oil}}\right] + \frac{h_k\,(x/0.4)\,H}{N_t} + C_{nf} \tag{6}$$

Three representative vessel classes were analyzed (Table 1). Engine power, efficiency, friction fraction, operating hours, and annual trip frequency were treated as scenario parameters informed by the technical ranges and vessel-class assumptions reported in the cited literature rather than by measurements from a probability sample of Indonesian fishing vessels. These parameters were selected to produce internally consistent BSFC values representative of small, medium, and larger vessels. Accordingly, absolute fuel consumption and cost estimates require recalibration using field data before operational application. The nominal fuel price was set at Rp6,800 per liter as a scenario assumption for subsidized diesel. Because the cited media source also reported a different price context for particular fishing-vessel categories, this value was not interpreted as a universally verified statutory price. Model users should instead substitute the fuel category, vessel class, policy period, and applicable subsidized price legally relevant to the target fleet. Uncertainty was propagated using 20,000 Latin hypercube samples across 13 parameters. The reported 90% simulation intervals corresponded to the 5th and 95th percentiles of the simulated output distributions rather than Bayesian credible intervals or frequentist confidence intervals. Global sensitivity was assessed using first-order and total-order Sobol indices calculated with the Saltelli estimator (Saltelli et al., 2010).

$$S_i = \frac{\mathrm{Var}_{X_i}[E(Y|X_i)]}{\mathrm{Var}(Y)}, \qquad S_{T,i} = \frac{E_{X_{\sim i}}[\mathrm{Var}(Y|X_{\sim i})]}{\mathrm{Var}(Y)} \tag{7}$$

RESULTS AND DISCUSSION

Results

Vessel Class Characteristics and Fuel Properties

Table 1 summarizes the parameters of the three vessel classes. Class A represents vessels of ≤5 GT equipped with 24-hp single-cylinder outboard or inboard engines and operating on daily trips. Class B represents 5–10-GT vessels equipped with 120-hp four-cylinder engines and operating on three-day trips. Class C represents 10–30-GT vessels equipped with 300-hp six-cylinder engines and operating on trips of approximately 10 days. Indicated efficiency and friction fraction were selected so that the cycle-average BSFC on neat diesel fell within the typical range for engines in each class, at 279, 246, and 226 g/kWh, respectively. These classes represent modeling scenarios rather than a statistically representative sample of the Indonesian fishing fleet. Consequently, comparisons among classes are useful for examining model behavior across different operating scales, whereas absolute fuel consumption, costs, and annual burdens should be validated against measured vessel data.

Table 1

Representative parameters of three fishing-vessel classes

Parameter	Class A (≤5 GT)	Class B (5–10 GT)	Class C (10–30 GT)
Rated power, P_r (kW)	17.9	88.0	220.0
Rated speed (rpm)	2,400	2,200	1,800
Indicated efficiency $\eta_{i,0}$ / friction fraction φ	0.36 / 0.15	0.40 / 0.13	0.43 / 0.12
Engine hours per trip h / trips per year N_t	10 / 200	30 / 70	120 / 25
Fuel cost share at B0, s_f	0.50	0.55	0.45
Filter cost (Rp) / interval (h)	75,000 / 500	250,000 / 500	600,000 / 500
Oil change cost (Rp) / interval (h)	120,000 / 250	600,000 / 250	1,800,000 / 250
Tank housekeeping H (Rp/year)	150,000	400,000	1,000,000
Baseline NOx, IMO Tier I (g/kWh)	9.80	9.80	10.05
Baseline CO / HC / PM (g/kWh)	4.5 / 1.5 / 0.90	3.0 / 0.9 / 0.60	2.0 / 0.6 / 0.40
E5-cycle BSFC at B0 (g/kWh)	279.1	245.7	226.0

Source: Compiled by the authors; baseline NOx values calculated using the IMO Tier I formula (IMO, 2008). The fuel price of Rp6,800/L is a nominal scenario input and should be replaced with the verified applicable subsidized price for the relevant vessel class and policy period in any field application.

Table 2 presents the blend properties calculated using Equations 1–2. At B40, the FAME volume fraction is 40%, whereas the calculated FAME mass fraction is 41.1% because FAME is denser than petroleum diesel. The mass-based lower heating value (LHV) decreases from 42.90 to 40.64 MJ/kg (−5.3%), whereas density increases by 1.9%, resulting in a decrease in volumetric energy content from 35.82 to 34.58 MJ/L (−3.46%). The energy-deficit parameter of neat biodiesel is $\theta = 0.0864$. The blend's oxygen content of approximately 4.6% by mass provides a plausible mechanism for improved oxidation. However, oxygen content alone does not determine the modeled magnitude of changes in CO, HC, or PM emissions; these estimates depend on the adopted emission-response functions and remain conditional on engine type, fuel-injection characteristics, and operating load.

Table 2

Calculated properties of blended fuels

Fuel	ρ (kg/L)	FAME mass fraction, w	LHV (MJ/kg)	E_v (MJ/L)	O_2 (% mass)
B0	0.835	0.000	42.90	35.82	0.0
B30	0.847	0.310	41.20	34.89	3.5
B40	0.851	0.411	40.64	34.58	4.6
B50	0.855	0.512	40.09	34.27	5.7

Source: calculated with Equations 1–2; FAME O_2 content assumed to be 11.2% by mass.

Analytical Proposition on Volumetric Consumption

Substituting Equations 2–4 yields Proposition 1. Within the Willans-line formulation adopted in this study, the ratio of blend fuel volume to neat-diesel fuel volume at equal brake power depends on θ, x, and δη (Equation 8). Because indicated efficiency enters the specified model as a uniform divisor across operating modes, the proportional volumetric penalty is invariant to the particular E5-cycle load weights under these assumptions. This is a property of the adopted model, not a universal characteristic of all fishing-vessel engines or operating cycles. Engines whose efficiency responses vary nonlinearly with load, speed, injection system, or transient operating conditions may exhibit different behavior.

$$\Delta_V(x) = \frac{V(x)}{V(0)} - 1 = \frac{1}{(1-x\theta)\left(1+\delta_\eta x/0.4\right)} - 1 \approx x\theta - \delta_\eta \frac{x}{0.4} \quad (8)$$

The second derivative of ΔV with respect to x is always positive (Equation 9), indicating that the consumption penalty is convex. Thus, each successive increase in blend level produces a slightly larger increase in fuel consumption than the preceding increase. With δη = 0, ΔV is 2.66% for B30, 3.58% for B40, and 4.52% for B50. With the nominal δη = −1% at B40, ΔV increases to 4.63%. Figure 1 shows that a ±2.5-percentage-point difference in the assumed efficiency change shifts the curve more substantially than the convexity effect itself. This finding provides an initial indication that combustion efficiency is the principal source of uncertainty.

$$\frac{\partial^2 \Delta_V}{\partial x^2}\Big|_{\delta_\eta=0} = \frac{2\theta^2}{(1-x\theta)^3} > 0 \quad (9)$$

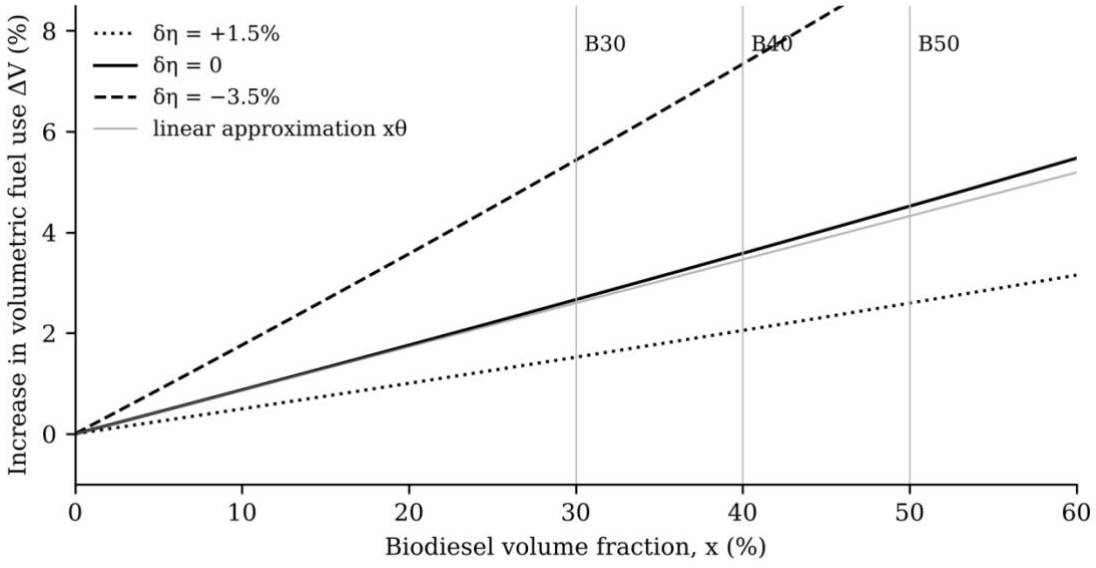


Figure 1. Increase in volumetric fuel consumption ΔV as a function of biodiesel fraction for three assumptions of the efficiency change δη at B40, compared with the linear approximation xθ

Engine Performance

Table 3 presents the engine performance indicators over the ISO 8178 E5 cycle. The 6.63% increase in mass-based BSFC is identical across the three modeled classes because the same blend-level LHV ratio and nominal relative efficiency change are applied to each class. Class-

specific baseline power and efficiency determine the absolute BSFC and fuel consumption per trip, but not the imposed proportional change. In simplified terms, BSFC is inversely proportional to the product of LHV and brake thermal efficiency. Therefore, the lower mass-based LHV (−5.3%), combined with the assumed 1.0% decline in efficiency, produces the same relative increase in BSFC across all three classes. Volumetric fuel consumption per trip subsequently combines mass-based fuel demand with blend density, resulting in a 4.63% increase in modeled fuel volume per trip for B40. Accordingly, mass-based BSFC and volume-based fuel demand should be interpreted as related but distinct effects.

Table 3
Engine performance indicators on the ISO 8178 E5 cycle (nominal values)

Class / Fuel	BSFC (g/kWh)	BTE (%)	V per trip (L)	ΔV (%)	ΔBSFC (%)
A – B0	279.1	30.1	20.49	–	–
A – B40	297.6	29.8	21.44	+4.63	+6.63
B – B0	245.7	34.2	266.02	–	–
B – B40	262.0	33.8	278.33	+4.63	+6.63
C – B0	226.0	37.1	2,446.80	–	–
C – B40	240.9	36.8	2,560.03	+4.63	+6.63
B – B50 (extension)	266.2	33.7	281.56	+5.84	+8.38

Source: simulation results; BTE = cycle-average brake thermal efficiency; nominal δη = −1% at B40.

Exhaust Emissions

Figure 2 illustrates the modeled changes in specific emissions per kWh for B30, B40, and B50, together with the 90% simulation interval for B40. At B40, CO emissions are estimated to decrease by 22.9% (simulation interval: −30.1% to −14.9%), HC emissions by 21.3% (−33.3% to −7.3%), and PM emissions by 22.6% (−29.9% to −14.6%). NOx emissions are estimated to increase by 4.9%, with an interval ranging from −0.5% to +10.6%. Thus, the model allows for both a small decrease and an increase, although 93.3% of the simulation draws yield positive changes. Fossil tank-to-wake CO_2 emissions decrease by 37.2% (−38.4% to −36.0%). This CO_2 estimate reflects only the reduced fossil-fuel fraction and the modeled change in fuel mass consumed. It is not a life-cycle greenhouse gas estimate and excludes palm cultivation, land-use change, FAME processing, and distribution. Likewise, the CO, HC, PM, and NOx values are model-based estimates rather than direct measurements from fishing vessels.

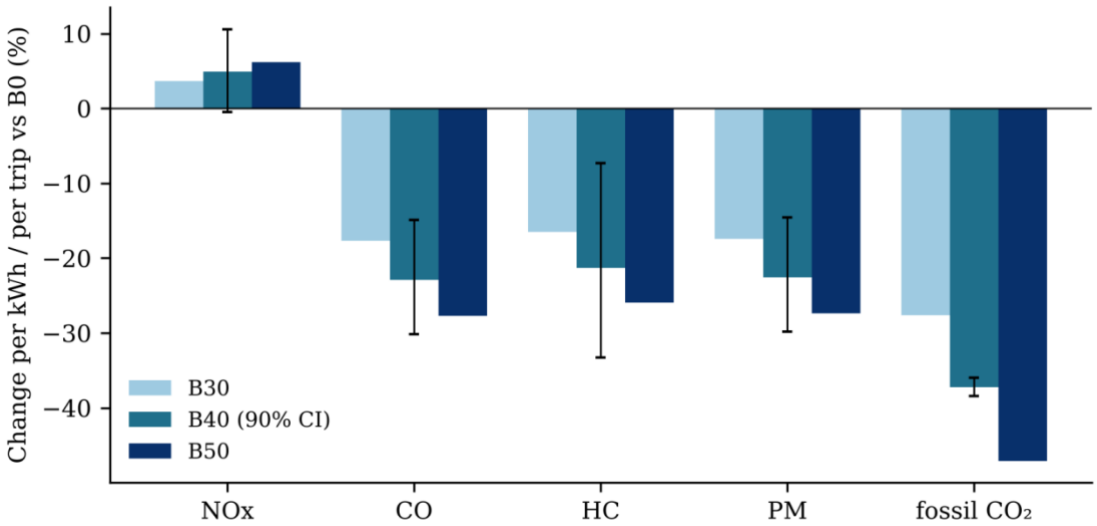


Figure 2. Change in specific emissions relative to B0 for B30, B40, and B50; error bars show the

Monte Carlo 90% simulation interval for B40

Operating Cost and Break-Even Price

The cost decomposition follows Equation 10. For each class, the fuel-cost contribution is approximated by multiplying the baseline fuel-cost share by the modeled increase in fuel volume, whereas the remaining contribution comes from filter, oil, and tank-housekeeping costs. Using the nominal values, additional fuel accounts for approximately Rp6.45 thousand of the Rp7.81 thousand increase for Class A (approximately 83%), Rp83.75 thousand of the Rp96.78 thousand increase for Class B (approximately 87%), and Rp770.4 thousand of the Rp889.2 thousand increase for Class C (approximately 87%). The remaining approximately 13–17% represents the combined modeled maintenance and housekeeping contributions. This decomposition demonstrates that changes in fuel volume are the dominant driver of the mean cost increase, whereas maintenance components remain operationally relevant even though their contributions to variance are smaller.

$$\frac{\Delta C(x)}{C_0} = s_f \, \Delta_V(x) + \frac{\Delta M(x)}{C_0} \tag{10}$$

Proposition 2 derives the per-liter price compensation, s*, required to make B40 cost-neutral (Equation 11). The first term represents energy compensation, whereas the second represents maintenance compensation per liter. At the nominal values, s* is Rp364/L for Class A, Rp348/L for Class B, and Rp347/L for Class C, equivalent to 5.1–5.4% of the pump price. The energy component alone amounts to Rp301/L across all three classes. For B50, s* increases to Rp433–454/L. The marginal transition from B40 to B50 adds 0.61–0.74% to the cost per trip.

$$s^*(x) = p - p^*(x) = \frac{p\,\Delta_V(x)}{1+\Delta_V(x)} + \frac{\Delta M(x)}{V(x)} \tag{11}$$

Table 4
Impact of B40 on operating cost and break-even compensation (nominal values and Monte Carlo 90% simulation intervals)

Indicator	Class A	Class B	Class C
Cost per trip at B0 (Rp)	278,680	3,288,957	36,973,825
ΔC per trip, B40 (Rp)	7,813	96,778	889,186
$\Delta C/C_0$ nominal (%)	2.80	2.94	2.40
$\Delta C/C_0$ median [90% simulation interval] (%)	2.84 [1.82, 3.94]	2.98 [1.88, 4.17]	2.45 [1.54, 3.43]
Annual ΔC, B40 (Rp million)	1.56	6.77	22.23
Break-even compensation s* B40 (Rp/L)	364 [245, 496]	348 [229, 477]	347 [230, 479]
Break-even compensation s* B50 (Rp/L)	454	433	433
Fossil CO_2 reduction per year (t)	4.04	18.36	60.30
Private abatement cost κ (Rp thousand/t CO_2)	387	369	369

Source: simulation results; values in square brackets are the 5th and 95th percentiles of 20,000 samples.

The private abatement cost, κ (Equation 12), defined here as the additional modeled cost borne by fishers per tonne of fossil tank-to-wake CO_2 emissions avoided, ranges from approximately Rp369 thousand to Rp387 thousand per tonne (approximately USD 22–24/t). Rennert et al. (2022) report a social cost of carbon estimate of USD 185/t. However, these two figures represent different concepts and accounting scopes: the former represents a private vessel-operating cost within this model, whereas the latter represents a monetized estimate of broader social climate damages. The comparison is therefore intended only to provide contextual

scale and should not be interpreted as evidence that the B40 policy generates a net social benefit.

$$\kappa(x) = \frac{\Delta C(x)}{M_{CO_2}(0) - M_{CO_2}(x)} \quad (12)$$

Uncertainty, Sensitivity, and Validation

Across all three modeled classes, each of the 20,000 parameter draws produced a positive operating-cost change under the specified probability distributions. This result indicates robustness within the sampled assumptions but does not imply absolute statistical certainty beyond the modeled parameter space. Class B exhibits the widest simulated distribution because it has the highest baseline fuel-cost share. Sobol sensitivity analysis identifies the assumed combustion-efficiency change as the dominant contributor to output variance, followed by fuel-cost share and biodiesel LHV. In contrast, maintenance parameters contribute relatively little to the variance in the modeled mean cost increase.

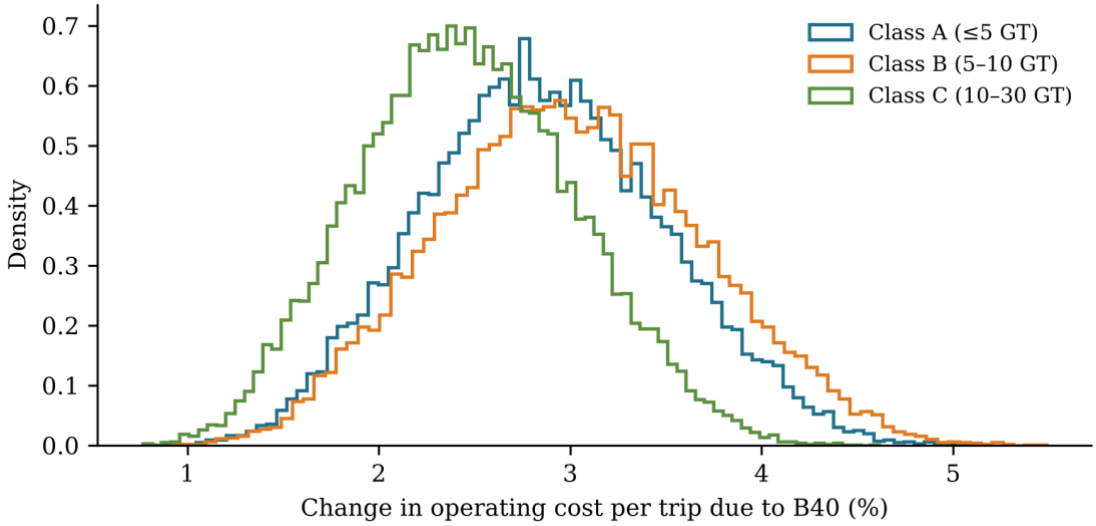


Figure 3. Monte Carlo distribution (n = 20,000) of the percentage increase in operating cost per trip due to B40 for three vessel classes

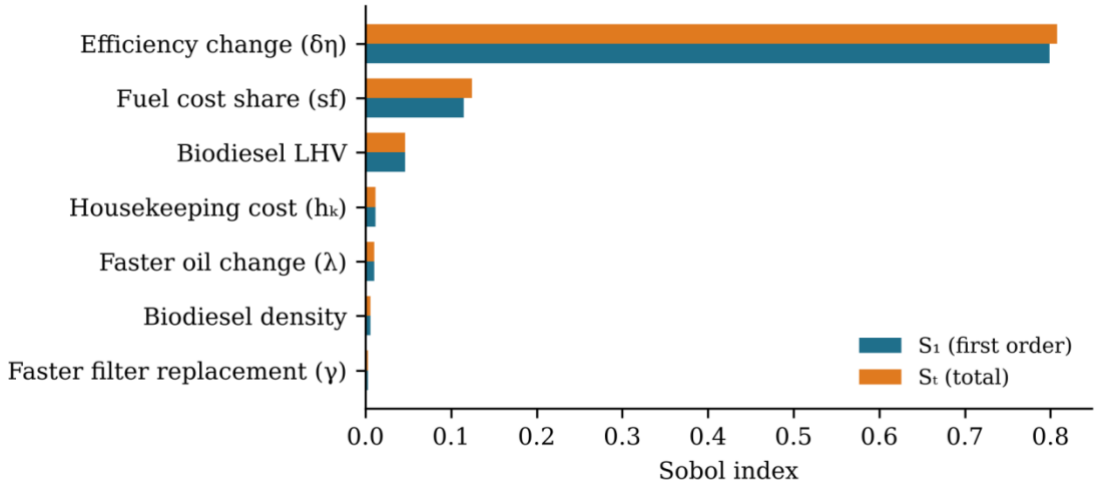


Figure 4. First-order and total Sobol indices for the percentage increase in Class B operating cost

Table 5 compares the model responses with available engine-test data for palm-based biodiesel blends. For B40, the reported changes in NOx, CO, and HC emissions fall within the model's 90% simulation intervals. For B20, the reported changes in thermal efficiency and BSEC fall outside the corresponding nominal modeled intervals. This comparison provides a limited

external plausibility check rather than a validation of fishing-vessel performance because the test engine and operating conditions differ from those of the representative vessel classes modeled in this study.

Table 5
External validation of model responses against engine test data for palm biodiesel blends

Indicator	Test data	Model: nominal [90% simulation interval]	Status
ΔNOx B40 (%)	+6.9	+4.9 [−0.5, +10.6]	Within CI
ΔCO B40 (%)	−24.0	−22.9 [−30.1, −14.9]	Within CI
ΔHC B40 (%)	−11.6	−21.3 [−33.3, −7.3]	Within CI
ΔBTE B20 (%)	−1.96	−0.5 [−1.75, +0.75]	Outside (conservative)
ΔBSEC B20 (%)	+2.12	+0.5 [−0.74, +1.78]	Outside (conservative)

Source: test data calculated from the g/kWh values and percentages in Musthafa & Prabhahar (2025); model values from this study's simulation.

Discussion

The main economic finding is that, at the assumed fixed pump price, the lower volumetric energy content of B40 creates an additional modeled cost burden equivalent to approximately Rp350/L in compensation. The term "implicit levy" is used solely as an economic metaphor for this unpriced burden; it does not refer to an official tax, statutory levy, or government charge. Under the stated Willans-line assumptions, Proposition 1 links this burden primarily to the difference between a price established per liter and the useful energy delivered per liter. This finding is consistent with reviews attributing the higher BSFC of biodiesel blends primarily to their lower heating value Xue et al. (2011), although the magnitude remains conditional on the assumed efficiency response and representative vessel parameters.

The dominance of δη in the Sobol decomposition (ST = 0.81) has both theoretical and practical implications. Theoretically, the effect of biodiesel on engine efficiency is ambiguous. A higher cetane number shortens ignition delay, while fuel-bound oxygen can improve combustion through enhanced oxidation. However, higher viscosity can impair fuel atomization, particularly in older engines equipped with mechanical injection systems (Lapuerta et al., 2008). The net effect depends on injection technology and engine condition. Therefore, uncertainty in δη is not necessarily a weakness of the model but rather reflects the actual heterogeneity of the fishing fleet. From a practical perspective, this finding establishes the priority for field research: measuring fuel consumption per trip and engine efficiency under actual fishing-vessel operating conditions is more important than further refining fuel-property data, which are already relatively well established. The B20 validation results, which indicate a greater efficiency decline than assumed in the nominal scenario, further support the possibility that actual operating costs may exceed the estimates presented here.

From an environmental perspective, the modeled B40 emission profile is broadly consistent with the literature reporting reductions in CO, HC, and PM emissions and a less consistent response in NOx emissions for biodiesel blends (Palash et al., 2013; Rizwanul Fattah et al., 2013). The 90% simulation interval for NOx includes both a small decrease and an increase. Therefore, the direction of the NOx response should not be considered certain across all engines. The modeled reduction in PM emissions may have potential local air-quality and public-health benefits in ports and coastal settlements. However, this study does not measure ambient pollutant concentrations, population exposure, or health outcomes. Accordingly, any health implications should be regarded as potential co-benefits requiring separate air-quality and epidemiological assessments rather than as directly demonstrated outcomes.

From a policy-economics perspective, the model quantifies the private operating-cost burden associated with the assumed fuel-price scenario. Any compensation mechanism, including the potential use of palm-oil-related funds, remains a policy option rather than a conclusion

established by the simulation. Implementation would require separate legal and institutional analyses addressing fund eligibility, subsidy regulations, target-vessel identification, administrative delivery, fiscal incidence, and safeguards against mistargeting. The break-even metric in Equation 11 therefore provides a transparent estimate of the compensation required to achieve modeled cost neutrality; it does not, by itself, establish the legal or administrative feasibility of any particular financing mechanism.

The convexity proposition (Equation 9) has direct implications for the transition from B40 to B50, which began in mid-2026. The marginal cost associated with each 10-percentage-point increase in biodiesel content rises, whereas the reduction in fossil CO_2 emissions per percentage point of biodiesel content remains approximately constant. Consequently, the marginal abatement cost of B50 is, on average, nearly the same as that of B40, although the absolute compensation required increases by approximately 25%. At the same time, non-energy-related operational risks may increase as the blend level rises. These risks include impaired fuel filterability near the cloud point, water uptake, and microbial growth in vessel fuel tanks (Dwivedi & Sharma, 2014). Although the model indicates that maintenance parameters contribute relatively little to the variance in average operating costs, these risks may have substantial consequences in extreme operational scenarios. A single clogged fuel filter at sea, for example, could jeopardize an entire fishing trip. Tank-housekeeping programs, water separators, and stabilizing additives developed for B40 Kirana Fadilah Achmad et al. (2025) should therefore be incorporated into the policy package, consistent with recommendations from studies on marine biodiesel use (Mohd Noor et al., 2018).

Theoretically, this study contributes to the socio-technical literature on energy transitions by demonstrating how a single physical parameter, the volumetric energy deficit θ, can translate deterministically into a distributional cost burden when fuel prices are set per unit of volume. The framework can be extended to other alternative fuels sold by volume but characterized by different energy contents, including hydrotreated vegetable oil (HVO) blends, which have demonstrated up to 2% better fuel economy than B40 in road tests (Mokhtar et al., 2023). The framework is also relevant to other biodiesel-producing countries with subsidized fishing fleets. More broadly, the findings contribute to the international debate on fisheries decarbonization, which has thus far focused more heavily on fleet efficiency Parker et al. (2018) than on the distributional consequences of fuel substitution.

This study has several limitations. First, the vessel-class and cost parameters represent illustrative scenarios rather than measurements obtained from a probability-based sample. Consequently, absolute fuel-consumption and cost estimates require recalibration using field data. Second, the emission-response functions are derived largely from land-based or controlled engine studies and may not fully represent the characteristics of small marine engines. Third, the quasi-steady-state model does not capture transient engine operation. Fourth, fossil CO_2 emissions are evaluated on a tank-to-wake basis and exclude upstream life-cycle emissions associated with palm cultivation, land-use change, FAME processing, and distribution. Future research should measure trip-level fuel consumption, engine efficiency, duty cycles, exhaust emissions, filter and oil replacement, tank and water-separator maintenance, fuel-storage conditions, and total operating costs on fishing vessels actually using B40. These observations should first be used to calibrate uncertain parameters, subsequently tested against an independent vessel sample for external validation, and ultimately integrated into a full life-cycle assessment to evaluate greenhouse gas outcomes beyond the tank-to-wake boundary.

CONCLUSION

This study presents an integrated modeling framework for estimating how B40 fuel properties, assumed changes in combustion efficiency, fuel consumption, literature-derived emission responses, maintenance requirements, and operating costs interact across three representative classes of Indonesian fishing vessels. Under the nominal assumptions, B40 reduces volumetric energy content by 3.46% and increases modeled fuel consumption by approximately 4.6% per trip, resulting in an operating-cost increase of approximately 2.4–3.0%. All 20,000 simulation draws produce a positive cost change within the specified parameter distributions; however, this finding should not be interpreted as absolute certainty beyond the modeled

parameter space. Fossil tank-to-wake CO_2 emissions are estimated to decrease by approximately 37%, while modeled CO, HC, and PM emissions decline by approximately 21–23%. The NOx estimate indicates an increase of approximately 5%, although its uncertainty interval includes a small decrease. These findings represent model-based estimates rather than direct vessel measurements or life-cycle greenhouse gas assessments.

The principal contributions of this study are the integrated performance–emissions–cost accounting framework, the analytical treatment of volumetric energy effects under explicit Willans-line assumptions, the development of a break-even cost-offset metric, and the sensitivity analysis identifying uncertainty in combustion efficiency as the principal driver of modeled cost variance. Accordingly, policy applications should initially prioritize field verification. Measurements of fuel consumption, engine efficiency, exhaust emissions, maintenance events, and vessel operating patterns are necessary to calibrate and independently validate the framework. Any compensation scheme should be evaluated separately in terms of its legal, institutional, and fiscal feasibility before implementation, particularly if the biodiesel mandate is increased toward B50.

ACKNOWLEDGMENTS

The authors would like to express their gratitude to the Universitas Muhammdiyah Surakarta, for the academic support provided throughout the conduct of this research. The authors also extend their appreciation to all parties who provided valuable input, suggestions, and support during the research process and manuscript preparation. The various contributions and feedback received have helped improve the quality, accuracy, and scientific presentation of this article, thereby enhancing its suitability for publication.

AUTHOR CONTRIBUTIONS

All authors contributed to the development of this research. Dimas Mahfud Baikuni Waluyo Adi Siswanto, as the first author, was responsible for initiating the research concept, developing the research framework, collecting and analyzing the data, interpreting the results, and preparing the initial manuscript draft. Amin Sulistyanto contributed to the development of the research ideas, academic supervision, methodological refinement, critical review of the manuscript's content, validation of the research findings, and final revision of the manuscript. All authors have read and approved the final version of the manuscript for publication and take responsibility for the integrity, accuracy, and transparency of all aspects of the research.

REFERENCES

Atabani, A. E., Silitonga, A. S., Badruddin, I. A., Mahlia, T. M. I., Masjuki, H. H., & Mekhilef, S. (2012). A comprehensive review on biodiesel as an alternative energy resource and its characteristics. *Renewable and Sustainable Energy Reviews*, *16*(4), 2070–2093. https://doi.org/10.1016/j.rser.2012.01.003

Dwivedi, G., & Sharma, M. P. (2014). Impact of cold flow properties of biodiesel on engine performance. *Renewable and Sustainable Energy Reviews*, *31*, 650–656. https://doi.org/10.1016/j.rser.2013.12.035

Fregolente, P. B. L., Fregolente, L. V., & Wolf Maciel, M. R. (2012). Water Content in Biodiesel, Diesel, and Biodiesel–Diesel Blends. *Journal of Chemical & Engineering Data*, *57*(6), 1817–1821. https://doi.org/10.1021/je300279c

Giakoumis, E. G., Rakopoulos, C. D., Dimaratos, A. M., & Rakopoulos, D. C. (2012). Exhaust emissions of diesel engines operating under transient conditions with biodiesel fuel blends. *Progress in Energy and Combustion Science*, *38*(5), 691–715. https://doi.org/10.1016/j.pecs.2012.05.002

Halimatussadiah, A., Nainggolan, D., Yui, S., Moeis, F. R., & Siregar, A. A. (2021). Progressive biodiesel policy in Indonesia: Does the Government's economic proposition hold? *Renewable and Sustainable Energy Reviews*, *150*, 111431. https://doi.org/10.1016/j.rser.2021.111431

Haryono, I., Suryantoro, M. T., Kurniawan, A., Ma'ruf, M., Rochmanto, B., Setiapraja, H., Rohman, A. T., Soewono, R. T., Yuwono, T., & Auzani, A. S. (2025). The Effect of Contaminants and

Temperatures of a High-Palm-Oil Biodiesel Blend on the Lifetime of a Diesel Fuel Filter. *Energies*, *18*(1), 219. https://doi.org/10.3390/en18010219

Haseeb, A. S. M. A., Fazal, M. A., Jahirul, M. I., & Masjuki, H. H. (2011). Compatibility of automotive materials in biodiesel: A review. *Fuel*, *90*(3), 922–931. https://doi.org/10.1016/j.fuel.2010.10.042

Hoekman, S. K., Broch, A., Robbins, C., Ceniceros, E., & Natarajan, M. (2012). Review of biodiesel composition, properties, and specifications. *Renewable and Sustainable Energy Reviews*, *16*(1), 143–169. https://doi.org/10.1016/j.rser.2011.07.143

Hoekman, S. K., & Robbins, C. (2012). Review of the effects of biodiesel on NOx emissions. *Fuel Processing Technology*, *96*, 237–249. https://doi.org/10.1016/j.fuproc.2011.12.036

International Maritime Organization. (2008). *Revised MARPOL Annex VI: Regulations for the prevention of air pollution from ships* (Resolution MEPC.176(58)).

International Organization for Standardization. (2020). *ISO 8178-4:2020 Reciprocating internal combustion engines — Exhaust emission measurement — Part 4: Steady-state and transient test cycles for different engine applications*.

Kalam, M. A., & Masjuki, H. H. (2002). Biodiesel from palmoil—an analysis of its properties and potential. *Biomass and Bioenergy*, *23*(6), 471–479. https://doi.org/10.1016/S0961-9534(02)00085-5

Kementerian Energi dan Sumber Daya Mineral. (2025). Wujudkan ketahanan energi dan kurangi impor, Menteri ESDM: Mandatori B40 berlaku 1 Januari 2025 [Achieving energy security and reducing imports, Minister of Energy and Mineral Resources: B40 mandate effective 1 January 2025] [Siaran pers]. https://www.esdm.go.id/id/media-center/arsip-berita/wujudkan-ketahanan-energi-dan-kurangi-impor-menteri-esdm-mandatori-b40-berlaku-1-januari-2025

Kirana Fadilah Achmad, A., Fathurrahman, N. A., Kunarti, E. S., Wibowo, C. S., Khalil, M., & Al-Saadi, A. A. (2025). Optimizing cold-flow properties and oxidation stability of B40 biodiesel blend with turpentine oil and ethanol: Experimental and quantum chemical approach. *Fuel*, *381*, 133258. https://doi.org/10.1016/j.fuel.2024.133258

Knothe, G. (2005). Dependence of biodiesel fuel properties on the structure of fatty acid alkyl esters. *Fuel Processing Technology*, *86*(10), 1059–1070. https://doi.org/10.1016/j.fuproc.2004.11.002

Lam, V. W. Y., Sumaila, U. R., Dyck, A., Pauly, D., & Watson, R. (2011). Construction and first applications of a global cost of fishing database. *ICES Journal of Marine Science*, *68*(9), 1996–2004. https://doi.org/10.1093/icesjms/fsr121

Lapuerta, M., Armas, O., & Rodríguez-Fernández, J. (2008). Effect of biodiesel fuels on diesel engine emissions. *Progress in Energy and Combustion Science*, *34*(2), 198–223. https://doi.org/10.1016/j.pecs.2007.07.001

Listrik Indonesia. (2026, July 13). B50 resmi dijual di SPBU Pertamina, berapa harganya? [B50 officially sold at Pertamina fuel stations: what is the price?]. https://listrikindonesia.com/detail/20613/b50-resmi-dijual-di-spbu-pertamina-berapa-harganya

Mohd Noor, C. W., Noor, M. M., & Mamat, R. (2018). Biodiesel as alternative fuel for marine diesel engine applications: A review. *Renewable and Sustainable Energy Reviews*, *94*, 127–142. https://doi.org/10.1016/j.rser.2018.05.031

Mokhtar, M., Sukmono, A., Setiapraja, H., Ma'ruf, M., Yubaidah, S., Haryono, I., Rochmanto, B., Soewono, R. T., Adhi Sukra, K. F., Thahar, A., Manurung, E., Wibowo, C. S., Widodo, S., Supriyadi, F., Abriyant, R. Y., Abriyant, R. Y., Suntoro, D., Faridha, F., & Reksowardojo, I. K. (2023). Towards nationwide implementation of 40% biodiesel blend fuel in Indonesia: a comprehensive road test and laboratory evaluation. *Biofuel Research Journal*, *10*(03), 1876–1889. https://doi.org/10.18331/BRJ2023.10.3.2

Musthafa, B., & Prabhahar, M. (2025). Numerical and experimental investigation of CI engine parameters using palm biodiesel with diesel blends. *Scientific Reports*, *15*(1), 43399. https://doi.org/10.1038/s41598-025-00170-8

Ong, H. C., Mahlia, T. M. I., Masjuki, H. H., & Norhasyima, R. S. (2011). Comparison of palm oil, Jatropha curcas and Calophyllum inophyllum for biodiesel: A review. *Renewable and*

Sustainable Energy Reviews, *15*(8), 3501–3515. https://doi.org/10.1016/j.rser.2011.05.005

Palash, S. M., Kalam, M. A., Masjuki, H. H., Masum, B. M., Rizwanul Fattah, I. M., & Mofijur, M. (2013). Impacts of biodiesel combustion on NOx emissions and their reduction approaches. *Renewable and Sustainable Energy Reviews*, *23*, 473–490. https://doi.org/10.1016/j.rser.2013.03.003

Parker, R. W. R., Blanchard, J. L., Gardner, C., Green, B. S., Hartmann, K., Tyedmers, P. H., & Watson, R. A. (2018). Fuel use and greenhouse gas emissions of world fisheries. *Nature Climate Change*, *8*(4), 333–337. https://doi.org/10.1038/s41558-018-0117-x

Passman, F. J. (2013). Microbial contamination and its control in fuels and fuel systems since 1980 – a review. *International Biodeterioration & Biodegradation*, *81*, 88–104. https://doi.org/10.1016/j.ibiod.2012.08.002

Pramudito, Y., Fathurrahman, N. A., Auzani, A. S., Wibowo, C. S., Anggarani, R., Soemanto, A., & Sugiarto, B. (2023). Comparative analysis of filterability behavior of B30 and B40 biodiesel blends on various porosity and dimension of fuel filter. *International Journal of Renewable Energy Development*, *12*(4), 760–767. https://doi.org/10.14710/ijred.2023.52801

Rennert, K., Errickson, F., Prest, B. C., Rennels, L., Newell, R. G., Pizer, W., Kingdon, C., Wingenroth, J., Cooke, R., Parthum, B., Smith, D., Cromar, K., Diaz, D., Moore, F. C., Müller, U. K., Plevin, R. J., Raftery, A. E., Ševčíková, H., Sheets, H., … Anthoff, D. (2022). Comprehensive evidence implies a higher social cost of CO2. *Nature*, *610*(7933), 687–692. https://doi.org/10.1038/s41586-022-05224-9

Rizwanul Fattah, I. M., Masjuki, H. H., Liaquat, A. M., Ramli, R., Kalam, M. A., & Riazuddin, V. N. (2013). Impact of various biodiesel fuels obtained from edible and non-edible oils on engine exhaust gas and noise emissions. *Renewable and Sustainable Energy Reviews*, *18*, 552–567. https://doi.org/10.1016/j.rser.2012.10.036

Sahara, Dermawan, A., Amaliah, S., Irawan, T., & Dilla, S. (2022). Economic impacts of biodiesel policy in Indonesia: a computable general equilibrium approach. *Journal of Economic Structures*, *11*(1), 22. https://doi.org/10.1186/s40008-022-00281-9

Saltelli, A., Annoni, P., Azzini, I., Campolongo, F., Ratto, M., & Tarantola, S. (2010). Variance based sensitivity analysis of model output. Design and estimator for the total sensitivity index. *Computer Physics Communications*, *181*(2), 259–270. https://doi.org/10.1016/j.cpc.2009.09.018

Tyedmers, P. H., Watson, R., & Pauly, D. (2005). Fueling Global Fishing Fleets. *AMBIO: A Journal of the Human Environment*, *34*(8), 635–638. https://doi.org/10.1579/0044-7447-34.8.635

Wirawan, S. S., Solikhah, M. D., Setiapraja, H., & Sugiyono, A. (2024). Biodiesel implementation in Indonesia: Experiences and future perspectives. *Renewable and Sustainable Energy Reviews*, *189*, 113911. https://doi.org/10.1016/j.rser.2023.113911

Xue, J., Grift, T. E., & Hansen, A. C. (2011). Effect of biodiesel on engine performances and emissions. *Renewable and Sustainable Energy Reviews*, *15*(2), 1098–1116. https://doi.org/10.1016/j.rser.2010.11.016